

Rough or crumpled: Phases in kinetic growth with surface relaxation

Sudip Mukherjee*

Barasat Government College, 10, KNC Road, Gupta Colony, Barasat, Kolkata 700124, West Bengal, India

Abhik Basu†

Theory Division, Saha Institute of Nuclear Physics,
1/AF Bidhannagar, Calcutta 700064, West Bengal, India

We show that generic kinetic growth processes with surface relaxations can exhibit a new crumpled phase with short-range orientational order at dimensions $d < 4$. A sufficiently strong spatially non-local part of the chemical potential associated with the particle current above a threshold in the system can trigger this crumpling. The system can also be in a perturbatively accessible rough phase with long range orientational order but short range positional order at $d < 4$ with known scaling exponents. Intriguingly, in $d > 4$ we argue that there is no crumpling transition; instead, there is a roughening transition from a smooth to a rough phase for large enough non-local particle current. Experimental and theoretical implications of these results are discussed.

Understanding of the large-scale properties like universal spatio-temporal scaling in condensed matter systems is a challenging problem from both theoretical and experimental perspectives. Significant Understanding has been made when these systems are at equilibrium [1], obeying a Fluctuation-Dissipation-Theorem (FDT) [2]. Studies on the scaling properties of fluctuating surfaces occupy a central position in statistical mechanics. *In-vitro* fluid or biomembranes and tethered membranes are two of the well-known equilibrium examples, which have been extensively studied [3]. Nonequilibrium surface fluctuations are far more difficult to analyse theoretically due to the combined effects of the nonlinear interactions and the lack of an FDT. The Kardar-Parisi-Zhang equation (KPZ) equation, originally proposed as a simple nonlinear model of nonconserved surface growth without any overhang [4, 5], provides a paradigmatic example of *roughening transition*, a nonequilibrium phase transition, between a *smooth* and a *rough* phase at dimensions $d > 2$. This rough phase is *perturbatively inaccessible*, i.e., cannot be captured by any systematic perturbation theory, but has been widely studied numerically [6]. A conserved version of the KPZ (CKPZ) equation driven by a conserved noise [7] has been proposed later that unsurprisingly belongs to a different universality class with no roughening transition at all. A subsequent generalisation of the CKPZ equation [8] reveals a more complex phase behaviour including roughening transitions in some region of the parameter space. A dynamical model that is closely related to the CKPZ equation is a nonlinear model used as a minimal description for Molecular Beam Epitaxy [5, 9] (here after the Lei-Das Sarma or LDS equation). It has the same conservation law structure as the CKPZ equation [7], but is driven by a nonconserved spatio-temporally white noise [5, 9]. Due to the difference in the noise statistics, the CKPZ and LDS equations be-

long to two different universality classes. Nevertheless, the surfaces that the CKPZ and LDS equations describe are either rough (for $d \leq 2(4)$ in case of the CKPZ (LDS) equation), or smooth in the other ranges of d .

In this Letter, we investigate the universal scaling in a generalised kinetic growth model with surface relaxation and a nonconserved noise, with a chemical potential μ having both local and non-local parts, associated with the particle current. This reduces to the LDS equation [9], when the non-local part μ vanishes. We show that for weaker non-local μ , the model belongs to the LDS universality class: At $d < 4$, it only has a rough phase whose exponents can be obtained in systematic renormalised perturbation expansions; the scaling exponents are identical to those obtained in Ref. [9]. For larger non-local μ , the surface however crumples at $d < 4$, as soon as the system size exceeds a finite threshold, with a concomitant loss of orientational long range order (LRO). This forms a novel nonequilibrium analogue of membrane crumpling, an intriguing phenomenon that is well-studied in the statistical mechanics of membranes in thermal equilibrium [10–13], but not in systems out of equilibrium. For $d > 4$, the model shows a *roughening transition* from a smooth to rough surfaces, controlled by the non-local part of μ , with the attendant loss of positional LRO.

We now derive these results. We start with the equation motion

$$\frac{\partial h}{\partial t} = -\nu \nabla^4 h - \frac{\lambda}{2} \nabla^2 (\nabla h)^2 - \lambda_1 \nabla \cdot [(\nabla h) \nabla^2 h] + \eta, \quad (1)$$

where $\nu > 0$ is a damping coefficients, $\eta(\mathbf{x}, t)$ is a Gaussian noise, and λ, λ_1 are the nonlinear coupling constants whose signs are arbitrary; $\lambda_1 = 0$ is the LDS equation [9]. Equation (1) has the form $\partial h / \partial t = -\nabla \cdot \mathbf{J} + \eta$, where current \mathbf{J} is given by

$$\mathbf{J} = \nu \nabla \nabla^2 h + \frac{\lambda}{2} \nabla (\nabla h)^2 - \lambda_1 (\nabla h) \nabla^2 h. \quad (2)$$

The first term of the rhs of (1), or equivalently, of (2), is a “curvature”-dependent part of the particle current at the

*Electronic address: sudip.bat@gmail.com

†Electronic address: abhik.123@gmail.com, abhik.basu@saha.ac.in

linear order in h . In fact, this term may be interpreted to have originated from the Helfrich free energy $F_H = (\nu/2) \int d^d x (\nabla^2 h)^2$ of a tensionless fluid membrane [2]. It contributes to (2) only if there is a gradient in the local mean curvature. Further, the two nonlinear terms with coefficients λ and λ_1 are the symmetry-permitted lowest order nonlinear terms, which are of nonequilibrium origin, and hence cannot be obtained from a free energy. Defining a chemical potential $\mu(\mathbf{x}, t)$ via $\mathbf{J} = \nabla \mu(\mathbf{x}, t)$ we find

$$\mu = \nu \nabla^2 h + \frac{\lambda}{2} (\nabla h)^2 + \lambda_1 \nabla^{-2} [(\nabla h) \nabla^2 h], \quad (3)$$

giving $\nabla^2 \mu = \nabla \cdot \mathbf{J}$. Thus, the λ_1 -term acts as a *non-local* chemical potential, as opposed to the local chemical potential term with coefficient λ . This λ_1 -term, originally introduced in Ref. [8] to generalise the CKPZ equation, can also been interpreted as “blind geodesic jumping” [8]. This λ_1 -term is responsible for a roughening transition in the generalised CKPZ equation, absent in the original version of the CKPZ equation, where $\lambda_1 = 0$ identically [8]. (Note that although we alluded to a fluid membrane in discussing the first term linear in h in the rhs of (1) or (2), the whole model equation (1) is not invariant under a tilt, and hence cannot describe a free-standing tensionless membrane.) The λ_1 -term has the same number of fields and gradients as the λ -term, and hence, both the terms are naively equally relevant in the renormalisation group (RG) sense [8]. Noise $\eta(\mathbf{x}, t)$ is zero-mean, Gaussian white noise with a variance

$$\langle \eta(\mathbf{x}, t) \eta(0, 0) \rangle = 2D\delta(\mathbf{x})\delta(t). \quad (4)$$

Universality of the statistical steady states of (1) are described by the universal spatio-temporal scaling of the time-dependent correlation function C of h :

$$C(r, t) \equiv \langle [h(\mathbf{x}, t) - h(0, 0)]^2 \rangle \sim r^{2\chi} f_h(r^z/t), \quad (5)$$

where, $r = |\mathbf{x}|$, χ_h and z , respectively, are the roughness and dynamic exponents.

RG analysis on the LDS equation shows that fluctuations modify the linear theory values of the scaling exponents at $d < 4$; it gives a rough phase with $\chi = \epsilon/3$ and $z = 4 - \epsilon/3$ to $\mathcal{O}(\epsilon)$ where $\epsilon \equiv 4 - d$ [9]. At $d > 4$, fluctuation-corrections are irrelevant and the linear theory values of the scaling exponents are obtained with $z = 4$ and $\chi = (4 - d)/2$. Thus $d = 4$ is the upper critical dimension of the LDS equation.

Is the λ_1 -term a relevant perturbation on the LDS equation? If so, what is the nature of the new steady state? We systematically examine these questions below. The nonlinear terms preclude exact enumeration of the scaling exponents. We therefore take a perturbative approach. Conservation law and the invariance under a constant shift of the base plane ensures that the fluctuations of h are long lived, such that the life-time of the fluctuations of size q^{-1} diverges as wavevector $q \rightarrow 0$. As a result, perturbative corrections to the model parameters diverge in the infra-red limit. These divergences are

systematically handled within the dynamic RG framework [5, 14–16]. The RG procedure is conveniently implemented by using a path integral description, equivalent to and constructed from Eq. (1) together with the noise variance (4), in terms of the field $h(\mathbf{x}, t)$, and its dynamic conjugate field $\hat{h}(\mathbf{x}, t)$ [16].

We perform one-loop Wilson momentum shell dynamic RG procedure, which is well-documented in the literature [5, 14, 15]. The resulting corrections to the model parameters are represented by the one-loop Feynman diagrams; see Supplemental Material (SM) [17]. There are *no* relevant fluctuation-corrections to the noise amplitude D , which is an *exact* statement. This is due to the fact that the noise in (1) is non-conserved, whereas the equation of motion (1) has the form of a conservation law. This means the corrections to D is at $\mathcal{O}(q^2)$, or higher, whereas the bare noise amplitude is $\mathcal{O}(q^0)$, ruling out any relevant (in the RG sense) corrections to it. Furthermore, there are no relevant one-loop corrections to λ or λ_1 [18]. There are however diverging one-loop corrections to ν . By dimensional analysis we identify two dimensionless effective coupling constants

$$g = \frac{\lambda^2 D}{\nu^3} K_d \Lambda^{d-4}, \quad \gamma = \frac{\lambda_1}{\lambda}. \quad (6)$$

Further g has a critical dimension $d_c = 4$ as in Ref. [9]. By following the standard steps of RG outlined in [5], we obtain the following differential RG recursion relation to the linear order in $\epsilon \equiv 4 - d$:

$$\frac{d\nu}{dl} = \nu[z - 4 + g\Delta(\gamma)], \quad (7)$$

$$\frac{d(\lambda, \lambda_1)}{dl} = (\lambda, \lambda_1)[\chi + z - 4], \quad (8)$$

$$\frac{dD}{dl} = D[z - d - 2\chi], \quad (9)$$

$$\frac{dg}{dl} = g[\epsilon - 3g\Delta(\gamma)], \quad (10)$$

where, $\Delta(\gamma) = \left(\frac{1}{8} - \frac{3\gamma^2}{8} + \gamma\right)$, $b \equiv \exp(l)$ is a length-scale; $\xi = b^\chi$, with χ being the roughness exponent; K_d is the surface area of a d -dimensional hypersphere of unit radius. With $\lambda_1 = 0$, (7) and (10) reduce to the flow equation for ν in the LDS equation [9]. The surface is rough or smooth, if $\chi > 0$ or < 0 . Since λ and λ_1 can have either sign independently of each other, the dimensionless ratio γ can also be positive or negative. Furthermore, since both λ and λ_1 *do not* renormalise at the one-loop order, their ratio $\gamma \equiv \lambda_1/\lambda$ too does not renormalise, and is *marginal*: $dg/dl = 0$.

Depending upon the signs of ϵ and Δ , there are four distinct cases obtained from $dg/dl = 0$ at the RG fixed point. We first focus on the cases with $\epsilon > 0$ (i.e., $d < 4$), which includes the physically relevant dimension 2.

(i) If $\epsilon > 0$ ($d < 4$) and $\Delta > 0$, then

$$g = 0, \quad g = \frac{\epsilon}{3\Delta} = g^*(\gamma) \quad (11)$$

as the fixed points of g . Out of these two fixed points, $g = g^*(\gamma)$ is stable. It is, in fact, a *fixed line* in the $g - \gamma$ plane, parametrised by γ . At this fixed line, by using $d\nu/dl = 0$, we get

$$z = 4 - g\Delta = 4 - \frac{\epsilon}{3}, \quad \chi = \frac{z - d}{2} = \frac{\epsilon}{3}. \quad (12)$$

These are identical to their counterparts in the LDS equation (i.e., $\gamma = 0$) [9], and form the LDS universality class. Thus, at this stable fixed point, valid when $\Delta > 0$ together with $\epsilon > 0$, model equation (1) belongs to the same universality class as that in Ref. [9] for all γ as long as $\Delta > 0$.

(ii) Now consider $\epsilon > 0$ ($d < 4$) and $\Delta < 0$. This gives

$$\frac{dg}{dl} = g[\epsilon + 3g|\Delta|]. \quad (13)$$

In this case, $g = 0$ is the only fixed point, which is unstable. We argue below that this represents crumpling of the surface.

We note that these two cases are distinguished by the sign of Δ . Naturally, $\Delta = 0$ gives the separatrix between the two kinds of behaviour, giving two solutions γ_1 and γ_2 for γ , or λ_1 in terms of λ :

$$\gamma_{1,2} = \frac{2}{3} \left[2 \pm \sqrt{19} \right] > (<)0, \quad (14)$$

$$\lambda_1 = \frac{2\lambda}{3} \left[2 \pm \sqrt{19} \right], \quad (15)$$

giving boundaries of stability in the $\lambda - \lambda_1$ plane; see Fig. 1(a) for a schematic phase diagram and discussions below. For $\gamma > \gamma_1$, or $\gamma < \gamma_2$, $\Delta < 0$, corresponding to case (ii), giving instability. In contrast, when γ belongs to the other range, i.e., $\gamma_1 > \gamma > \gamma_2$, $\Delta > 0$, we get $g = g^*(\gamma) = \epsilon/(3\Delta)$ as the stable fixed point. As noted earlier, the stable case (i) belongs to the same universality class of Ref. [9]. The unstable case (ii) is *new*, and is due to the nonlinear term with coefficient λ_1 in Eq. (1). Since γ is *marginal* at the one-loop order (which is the order of the perturbation theory here), we obtain a *fixed line* in the $g - \gamma$ plane in the stable case. In fact, from (11), if $\gamma = 0$, unsurprisingly the LDS fixed point is recovered: $g^*(\gamma = 0) = 8\epsilon/3$. For $\gamma_1 > \gamma \geq 0$, we note that initially, for very small $\gamma > 0$, $g^*(\gamma)$ *decreases* as γ rises, but eventually starts to rise as γ crosses a threshold $\gamma_1^* = 4/3$, which maximises Δ , and diverges as $\gamma \rightarrow \gamma_1$ from below. Thus g^* has a nonmonotonic dependence on γ when $\gamma_1 > \gamma \geq 0$. We find that $g^*(\gamma = \gamma_1^*) = 19\epsilon/24$, which is the smallest value of g^* possible. In contrast, in the range $\gamma_2 < \gamma < 0$, g^* rises monotonically as γ decreases, eventually diverging as $\gamma \rightarrow \gamma_2$ from above. Since γ is marginal in the one-loop approximation, within the range $\gamma_2 < \gamma < \gamma_1$ the RG flow lines flow parallel to the g -axis towards the “fixed line” described above. Outside this regions, the flow lines flow parallel to the g -axis towards infinite g , indicating breakdown of the perturbation theory. See Fig. 1(b) for a schematic RG flow diagram in the $g - \gamma$ plane.

We can solve Eq. (13) to get

$$g(l) = \frac{\epsilon}{3|\Delta|} \frac{A \exp(\epsilon l)}{1 - A \exp(\epsilon l)}. \quad (16)$$

The constant of integration A can be evaluated by using the “initial” condition: at $l = 0$, $g(0) = g_0$. This gives $A = (g_0/\epsilon)3|\Delta| + g_0$. If $\Delta \rightarrow 0$ from below, we get $A \approx g_0(\frac{3|\Delta|}{\epsilon})$, corresponding to $g(l) \approx g_0 e^{\epsilon l}$, giving the initial growth of $g(l)$ before the nonlinear effects become important. For any finite $\Delta < 0$, $g(l)$ diverges at a finite $l = l_c$ if $1 - A \exp(\epsilon l_c) \rightarrow 0_+$, giving $l_c = \frac{1}{\epsilon} \ln A$ as the critical “RG time” at which $g(l)$ diverges.

We now use (16) to obtain the scale-dependent renormalised $\nu(l)$. Substituting $g(l)$ in (7), we find

$$\nu(l) = \nu_0 \exp \left[-\frac{\epsilon}{3} \int dl \frac{A \exp(\epsilon l)}{1 - A \exp(\epsilon l)} + (z - 4)l \right], \quad (17)$$

which clearly shows that $\nu(l)$ vanishes as $l \rightarrow l_c \sim \mathcal{O}(1)$ from below, or equivalently, as the length-scale dependent $\nu(L)$ vanishes as $L \rightarrow \xi$ from below, where $\xi = a_0 \exp(l_c)$; a_0 is a small-scale cutoff. We thus identify ξ as the *persistence length*, beyond which the system crumples. Of course, the perturbation theory actually breaks down as soon $g(l)$ becomes $\mathcal{O}(1)$.

We now argue that case (ii) represents a *crumpled phase*, quite distinct from a rough surface. A rough surface is characterised by (a) a positive $\chi > 0$, which implies $\langle h^2(\mathbf{x}, t) \rangle$ growing with the system size L , which in turn implies a lack of positional LRO, together with (b) a finite (i.e., L -independent in the limit of large L) $\langle (\nabla h)^2 \rangle$ meaning *orientational LRO*. For instance, in the LDS equation, $\chi = \epsilon/3 > 0$. Therefore, $\langle h^2(\mathbf{x}, t) \rangle \sim L^{2\epsilon/3}$, growing indefinitely with L . On the other hand, $\langle (\nabla h)^2 \rangle$ remains L -independent. In contrast, a crumpled surface not only lacks positional LRO, it *also lacks orientational LRO*. This is reflected in the divergence of $\langle (\nabla h)^2 \rangle$ in the limit of large L . It is clear that the LDS rough surfaces are *not* crumpled, since $\langle (\nabla h)^2 \rangle$ remains L -independent, which is similar to the equilibrium tethered membranes in their low temperature (T) orientationally ordered phase [10]. In contrast, finite but sufficiently large two-dimensional (2D) equilibrium fluid or lipid membranes necessarily crumple at any non-zero temperature [2, 19]. Thus a rough (but non-crumpled) and a crumpled surface are distinguished by the presence or absence of long-range orientational order. While the phenomenon of crumpling should be rather generic, independent of the conditions of equilibrium, a nonequilibrium example of crumpling in a growing surface has not yet been found.

We further note that in the crumpled phase of the present study, the fluctuation-corrections to ν are *negative*, meaning $\nu(l)$ vanishes in a finite RG time $l_c = \ln(\xi/a_0)$; see (17) above. Indeed, at this stage we can make a formal connection with the crumpling of equilibrium statistical mechanics of fluid membranes. Notice that D/ν_{eff} has the direct correspondence with T/κ_{eff} of

the membrane, where κ_{eff} is an “effective” bend modulus of the membrane, and ν_{eff} is the fluctuation-corrected, effective ν of the surface, calculated in the bare perturbation theory. In case of fluid [19, 20] or asymmetric tethered [11, 12] membranes, κ_{eff} , and along with *both* $\langle h^2(\mathbf{x}, t) \rangle$ and $\langle (\nabla h)^2 \rangle$ diverge as soon as the membrane size exceeds a finite threshold, a telltale signature of crumpling. Likewise here, ν_{eff} vanishes and along with it *both* $\langle h^2(\mathbf{r}, t) \rangle$, and $\langle (\nabla h)^2 \rangle$ diverge, as soon as the system size exceeds a finite threshold, giving a nonequilibrium crumpling. Clearly, the surface morphology in the crumpled phase is fundamentally different from that in the rough phase in the LDS equation.

We thus find that in the $\lambda - \lambda_1$ plane, for $d < 4$ (15) gives the boundaries between regions with a rough phase belonging to the LDS universality class, and a crumpled phase; see the schematic phase diagram in Fig. 1(a). We further show the RG flow lines ($d < 4$) in the $g - \gamma$ plane in Fig. 1(b). Flow lines run parallel to the g axis. For $\gamma_2 < \gamma < \gamma_1$, flow lines approach a *fixed line*, whose each point corresponds to the LDS universality class. Outside this window, the flow lines run to infinity along the g direction, indicating crumpling of the surface.

We have found that $g^* \rightarrow \infty$ as $\gamma \rightarrow \gamma_1(\gamma_2)$ from below (above). However, long before g diverges, our perturbation theory breaks down. In fact, it loses validity as soon as $g^* \sim \mathcal{O}(1)$. While we cannot obviously follow the RG flows all the way to infinity, we can speculate about the nature of the phases in the region of the parameter space where the RG flow lines appear to run

away to infinity. For this, we are guided by the general understanding that for large enough noise any system, equilibrium or nonequilibrium, should undergo a phase transition from a low-noise “ordered phase” to a high noise “disordered phase”. Accordingly, the physical expectation in the present model is that for large enough g (which here means large enough noise or D), the system at $d < 4$ undergoes a phase transition from a low-noise orientationally ordered rough phase to a phase with SRO only (i.e., no orientational LRO), i.e., the crumpled phase. Thus, upon increasing g , the rough phase ($d < 4$) should be unstable, and the surface should eventually crumple. This should hold even in the original LDS equation ($\gamma = 0$), for sufficiently g : we expect an unstable “crumpling fixed point” beyond which the RG flow runs away to infinity signalling loss of orientational LRO. Accordingly, there must be an unstable critical point on the g -axis, controlling this transition to this putative crumpled phase. If we now consider the full RG flows for a surface in the two dimensional parameter space (g, γ) and connect this putative flow with our flows for small g and γ in the simplest possible way (i.e., one that does not involve introducing any other new fixed points), we are then led to Fig. 1(c). This is basically an “Occam’s razor”-style argument: Fig. 1(c) has the simplest flow topology that naturally reduces to the known flow trajectories for small g, γ (as shown in Fig. 1(b)). At the same time, it gives the putative global flow lines, allowing for a transition to a presumed crumpled phase.

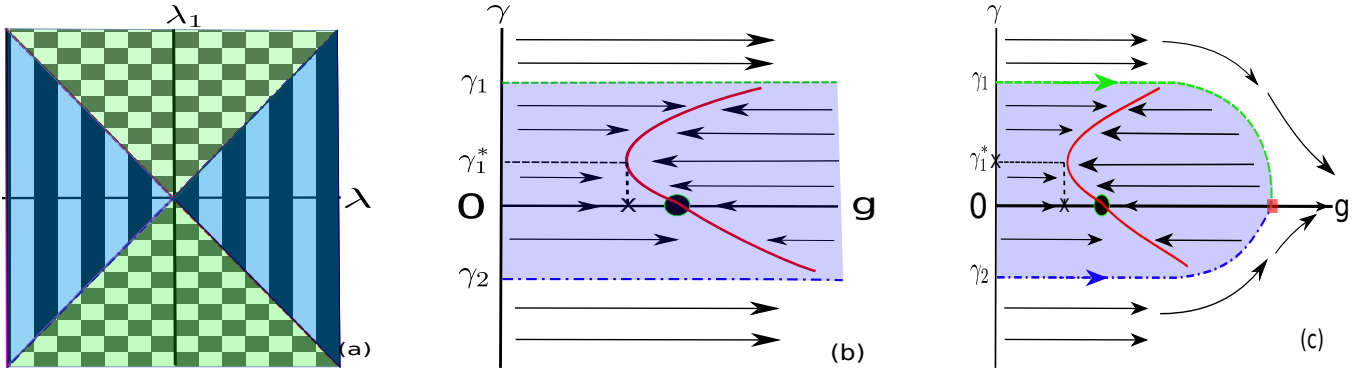


FIG. 1: (colour online)(a) Schematic phase diagram in the $\lambda - \lambda_1$ plane ($d < 4$), showing the regions (stripes) corresponding to a rough (stripes) and a crumpled (checkerboard) phase. (b) Schematic phase diagram and the RG flow lines in the $g - \gamma$ plane ($d < 4$). The small filled circle on the g -axis is the original LDS fixed point $g = 8\epsilon/3$. The red curved line is the *fixed line* $g = \epsilon/(3\Delta(\gamma))$. (c) Conjectured “Occam’s razor” global RG flows in the $g - \gamma$ -plane ($d < 4$). Arrows indicate the flow directions. The green and blue broken lines give the boundary between the stable (rough) and the crumpled phases. The small filled red square on the g -axis is the putative unstable fixed point not accessible in our perturbative RG (see text).

We now consider the cases with $d > 4$ (i.e., $\epsilon < 0$), which although are not physically accessible, provide interesting theoretical insights.

(iii) Consider now $\epsilon < 0$ ($d > 4$) and $\Delta < 0$. This gives

$$\frac{dg}{dl} = g [-|\epsilon| + 3g|\Delta|], \quad (18)$$

giving $g^* = 0$ as the stable fixed point for a *smooth phase* with positional LRO, and $g^* = |\epsilon|/(3|\Delta(\gamma)|)$ as the unstable fixed line, parametrised by γ . This is reminiscent of a roughening transition of the KPZ equation [5]. We also note that the fluctuation-corrections to ν remain finite even for $L \rightarrow \infty$ for $d > 4$, which rules out vanishing of ν_{eff} , in turn precluding crumpling. Instead, we obtain a roughening transition between a smooth phase ($g^* = 0$) and a perturbatively inaccessible rough phase, akin to the roughening transition in the KPZ equation at $d > 2$ [5].

(iv) Finally, for $\epsilon < 0$ ($d > 4$) and $\Delta > 0$

$$\frac{dg}{dl} = g[-|\epsilon| - 3g\Delta], \quad (19)$$

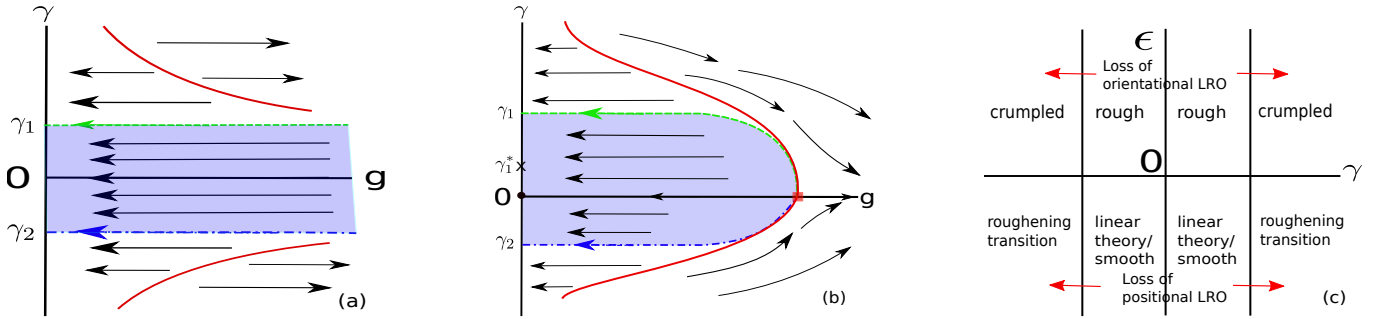


FIG. 2: (colour online) (a) Schematic phase diagram and the RG flow lines in the $g - \gamma$ plane ($d > 4$). The red curved lines are the *unstable fixed lines* given by $g = \epsilon/3|\Delta|$, $\Delta < 0$. The shaded region has only a smooth phase; elsewhere there is a roughening transition, (b) Conjectured ‘Occam’s razor’ global RG flows in the $g - \gamma$ -plane ($d > 4$). Arrows indicate the flow directions. The red curved lines are the *unstable fixed lines* that reduces to $g = \epsilon/3|\Delta|$, $\Delta < 0$, in the lowest order perturbation theory. (c) Phases in the $\gamma - \epsilon$ plane. Loss of order across the transitions is shown (see text).

For $d > 4$, (15) give the boundaries between smooth phase ($\chi < 0$) and roughening transition to a perturbatively inaccessible rough phase akin to the rough phase of the KPZ equation for $d > 2$.

The four distinct cases depending upon γ and ϵ are schematically shown in Fig. 2(c).

To summarise, we have uncovered an intriguing crumpling instability in $d < 4$ in addition to the well-known perturbatively-accessible rough phase which is controlled by the LDS fixed point, by suitably generalising the LDS equation. The crumpling is controlled by the relative strength of a spatially non-local chemical potential vis-à-vis the corresponding local part. We further show that for $d > 4$, instead of a crumpling transition, the system undergoes a roughening transition for a sufficiently large non-local particle current, which is akin to the roughening transition of the KPZ equation at $d > 2$. We argue that in order to distinguish between a rough (having orientational LRO) and a crumpled surface (with SRO), one must measure the variance $\langle(\nabla h)^2\rangle$ of the orientation fluctuations, which for a rough surface is *finite* in thermodynamic limit, but diverges for a crumpled surface.

giving $g^* = 0$ is the only fixed point, that is stable.

The RG flow for cases (iii) and (iv) are shown in Fig. 2(a). We could again apply an Occam’s razor style argument as above. Unlike $d < 4$, we now expect loss of positional LRO of the smooth phase upon increasing g , resulting into transitions to a rough phase with no positional LRO (but with orientational LRO): we assume a putative unstable roughening fixed point in the g -axis for high enough g , and arrive at the putative global RG flow diagram shown in Fig. 2(b). For $d > 4$, Fig. 1(a) gives the phase boundaries between regions having only smooth phases with no phase transitions and regions with roughening transitions.

This fact should be kept in mind in any future numerical studies of this problem.

As has been discussed in Ref. [9], one could potentially add a term of the form $\nabla \cdot (\nabla h)^3$ in (1), which generates a $\nabla^2 h$ -term in (1) by RG. As in Ref. [9], we ignore this term here. Our results indicate the generic difficulty associated with the production of flat thin films, since for large λ_1 , the surface crumples. One might have large patches in the system characterised by λ_1 , with some having λ_1 large enough to trigger crumpling in local patches, which may in turn ultimately destroy the film. It would be interesting to construct microscopic models, which may be used to relate λ_1 with the underlying microscopic processes, thereby gaining further useful insight. We hope our studies will provide impetus to future theoretical studies on nonequilibrium crumpling.

Acknowledgement:- S.M. thanks the SERB, DST (India) for partial financial support through the TARE scheme [file no.: TAR/2021/000170] (2022). A.B. thanks the SERB, DST (India) for partial financial support through the MATRICKS scheme [file no.: MTR/2020/000406] (2021).

[1] D. Jasnow, Phase transitions and critical phenomena, edited by J. L. Lebowitz and C. Domb, Vol. 17 (Academic Press, London, 1986).

[2] P. M. Chaikin and T. C. Lubensky, Principles of condensed matter physics, Vol. 1 (Cambridge University Press, Cambridge, 2000).

[3] D. R. Nelson, T. Piran, and S. Weinberg, Statistical Mechanics of Membranes and Surfaces (World Scientific, Singapore, 2004), DOI: 10.1142/5473.

[4] M. Kardar, G. Parisi and Y-C. Zhang, Dynamic Scaling of Growing Interfaces, *Phys. Rev. Lett.*, **56**, 889 (1986).

[5] A-L Barabási and H. E. Stanley, Fractal concepts in surface growth (Cambridge university press, 1995).

[6] T. Halpin-Healy and K-C. Zhang, Kinetic roughening phenomena, stochastic growth, directed polymers and all that, *Phys. Rep.* 254, 215 (1995); A. Basu and E. Frey, “Novel universality classes of coupled driven diffusive systems,” *Phys. Rev. E* 69, 015101 (2004); A. Basu and E. Frey, Scaling and universality in coupled driven diffusive models, *J. Stat. Mech.: Theory Exp.* 2009, P08013 (2009).

[7] T. Sun, H. Guo and M. Grant, Dynamics of driven interfaces with a conservation law, *Phys. Rev. A* 40, R6763 (1989).

[8] F. Caballero et al, Strong Coupling in Conserved Surface Roughening: A New Universality Class?, *Phys. Rev. Lett.* 121, 020601 (2018).

[9] Z. -W. Lai and S. Das Sarma, Kinetic Growth with Surface Relaxation: Continuum versus Atomistic Models, *Phys. Rev. Lett.* **66**, 2348 (1991).

[10] M. Paczuski, M. Kardar, and D. R. Nelson, Landau Theory of the Crumpling Transition, *Phys. Rev. Lett.* 60, 2638 (1988).

[11] T. Banerjee, N. Sarkar, J. Toner, and A. Basu, Rolled up or Crumpled: Phases of Asymmetric Tethered Membranes, *Phys. Rev. Lett.* 122, 218002 (2019).

[12] T. Banerjee, N. Sarkar, J. Toner and A. Basu, Statistical mechanics of asymmetric tethered membranes: Spiral and crumpled phases, *Phys. Rev. E* 99, 053004 (2019).

[13] F. David and E. Guitter, Crumpling Transition in Elastic Membranes: Renormalization Group Treatment, *Europhys. Lett.* **5**, 709 (1988).

[14] D. Forster, D. R. Nelson, and M. J. Stephen, Large-distance and long-time properties of a randomly stirred fluid, *Phys. Rev. A* **16**, 732 (1977).

[15] P. C. Hohenberg and B. I. Halperin, Theory of dynamic critical phenomena, *Rev. Mod. Phys.* **49**, 435 (1977).

[16] R. Bausch, H. Janssen, and H. Wagner, Renormalized field theory of critical dynamics, *Z. Phys. B* **24**, 113 (1976); U. Täuber, Critical Dynamics (Cambridge University Press, Cambridge, 2014).

[17] See Supplemental Material for details of the RG calculations including the Feynman diagrams.

[18] H. Janssen, On Critical Exponents and the Renormalization of the Coupling Constant in Growth Models with Surface Diffusion, *Phys. Rev. Lett.* **78**, 1082 (1997).

[19] L. Peliti and S. Leibler, Effects of Thermal Fluctuations on Systems with Small Surface Tension, *Phys. Rev. Lett.* 54, 1690 (1985).

[20] T. Banerjee and A. Basu, Thermal fluctuations and stiffening of symmetric heterogeneous fluid membranes, *Phys. Rev. E* **91**, 012119 (2015).

Appendix A: Action functional

Model equation (1) can be written down as a path integral over configurations given by $h(\mathbf{x}, t)$ and its dynamic conjugate $\hat{h}(\mathbf{x}, t)$, which can be used to conveniently calculate the various correction and vertex functions in the

problem. The generating functional is given by

$$\mathcal{Z} = \int \mathcal{D}h \mathcal{D}\hat{h} \exp(-S), \quad (\text{A1})$$

where S is the action functional given by

$$S = \int d^d r dt \left[-D\hat{h}(\mathbf{r}, t)\hat{h}(\mathbf{r}, t) \right] + \int d^d x dt \hat{h} \left[\partial_t h + \nabla^2 \left\{ \nu \nabla^2 h + \frac{\lambda}{2} (\nabla h)^2 \right\} + \lambda_1 \nabla \cdot \{ (\nabla^2 h) \nabla h \} \right]. \quad (\text{A2})$$

We can now write down the “bare” two-point correlation functions in the problem by using (A1) and the harmonic or Gaussian part of (A2); i.e., by setting $\lambda = 0 = \lambda_1$. We obtain

$$\langle |\hat{h}(\mathbf{q}, \omega)|^2 \rangle = 0, \quad (\text{A3})$$

$$\langle \hat{h}(-\mathbf{q}, -\omega) h(\mathbf{q}, \omega) \rangle = \frac{1}{-i\omega + \nu q^2}. \quad (\text{A4})$$

$$\langle |h(\mathbf{q}, \omega)|^2 \rangle = \frac{2D}{\omega^2 + \nu^2 q^4}. \quad (\text{A5})$$

Appendix B: Renormalisation group analysis

We outline here the basic steps of the RG calculations performed in the main text. The RG is done by tracing over the short wavelength Fourier modes of the fields $h(\mathbf{x}, t)$ and $\hat{h}(\mathbf{x}, t)$ [5, 14, 15]. In particular, we follow the usual approach of initially restricting the wavevectors to be within a bounded spherical Brillouin zone: $|\mathbf{k}| < \Lambda$. However, the precise value of the upper cutoff Λ has no effect on our final results. The fields $h(\mathbf{r}, t)$ and $\hat{h}(\mathbf{r}, t)$ are separated into the high and low wave vector parts: $h(\mathbf{r}, t) = h^<(\mathbf{r}, t) + h^>(\mathbf{r}, t)$, $\hat{h}(\mathbf{r}, t) = \hat{h}^<(\mathbf{r}, t) + \hat{h}^>(\mathbf{r}, t)$, where $h^>(\mathbf{r}, t)$ and $\hat{h}^>(\mathbf{r}, t)$ have support in the large wave vector (short wavelength) range $\Lambda e^{-l} < |\mathbf{k}| < \Lambda$, while $h^<(\mathbf{r}, t)$ and $\hat{h}^<(\mathbf{r}, t)$ have support in the small wave vector (long wavelength) range $|\mathbf{k}| < e^{-l} \Lambda$; $b \equiv e^l > 1$.

We then integrate out $h^>(\mathbf{r}, t)$ and $\hat{h}^>(\mathbf{r}, t)$ in the anhamonic coupling λ and λ_1 ; as usual, this resulting perturbation theory of $h^<(\mathbf{r}, t)$, $\hat{h}^<(\mathbf{r}, t)$ can be represented by Feynman graphs, with the order of perturbation theory reflected by the number of loops in the graphs we consider. We restrict ourselves here up to the one-loop order. After this perturbative step, we rescale lengths, with $\mathbf{r} \rightarrow \mathbf{r}' e^l$, which restores the UV cutoff back to Λ , together with rescaling of time $t \rightarrow t' e^{zl}$ (equivalently in the Fourier space, the momentum and frequency are rescaled as $\mathbf{k} \rightarrow \mathbf{k}'/b$ and $\omega \rightarrow \omega'/b^z$, respectively), where z is the dynamic exponent. This is then followed by rescaling the long wave length part of the fields that we define in the Fourier space for calculational convenience. We scale $h^<(\mathbf{q}, \omega) = \xi h(b\mathbf{q}, b^z \omega)$, $\hat{h}^<(\mathbf{q}, \omega) = \hat{\xi} \hat{h}(b\mathbf{q}, b^z \omega')$. T

Next, we set $\xi \hat{\xi} = b^{d+2z}$ by demanding the term in action (A2) $\int d^d \mathbf{k} d\omega \hat{h} h \omega$ does not scale with momentum scaling. Accordingly the model parameters scale below:

$$\nu' = \nu^< b^{z-4}, D'_h = D_h^< b^{z-d-2\chi_h}, \quad (\text{B1})$$

$$(\lambda', \lambda'_1) = (\lambda^<, \lambda_1^<) b^{z-2+\chi}. \quad (\text{B2})$$

1. One-loop Feynman diagrams for ν

2. One-loop vertex corrections

Sum of these diagrams in Fig. (5) vanishes.

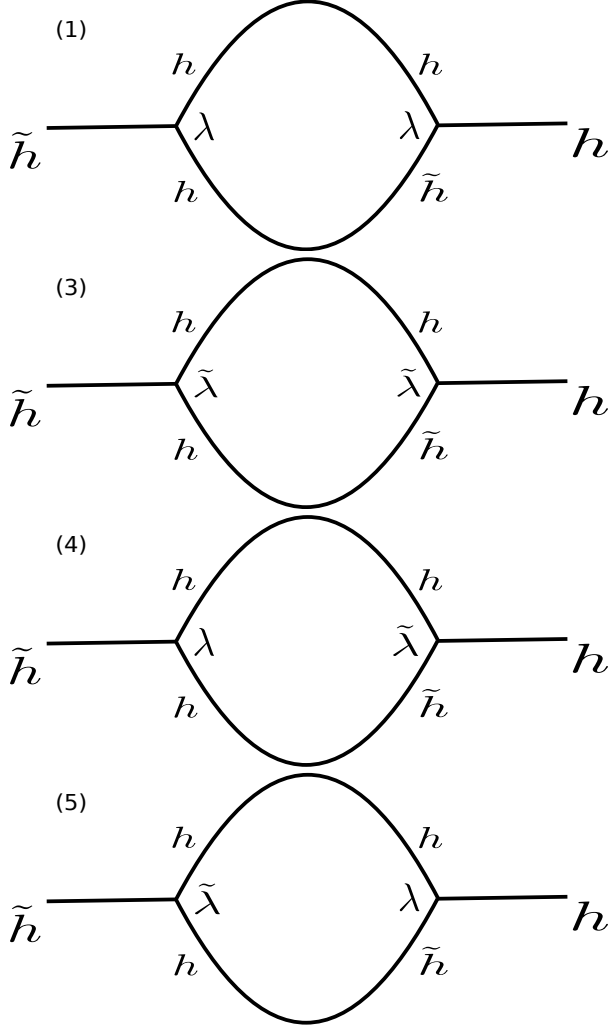


FIG. 3: One-loop Feynman diagrams which contribute to the fluctuation-correction of ν .

Sum of these diagrams in Fig. (6) vanishes.

Appendix C: Perturbative corrections to the model parameters

Combining all the diagrams in Fig. (3), and evaluating them, we obtain the fluctuation-correction diffusivity $\nu^<$:

$$\begin{aligned} \nu^< = & \nu \left[1 + \frac{\lambda^2 D}{\nu^3} \frac{6-d}{4d} K_d \int_{\Lambda/b}^{\Lambda} dq q^{d-5} \right. \\ & - \frac{\lambda_1^2 D}{\nu^3} K_d \int_{\Lambda/b}^{\Lambda} dq q^{d-5} \\ & \left. + \frac{\lambda_1^2 D}{\nu^3 d} \left(\frac{6-d}{4} - \frac{6}{d+2} + 3 \right) K_d \int_{\Lambda/b}^{\Lambda} dq q^{d-5} \right] \end{aligned}$$

$$+ \frac{\lambda \lambda_1 D}{\nu^3} K_d \int_{\Lambda/b}^{\Lambda} dq q^{d-5} \Big], \quad (C1)$$

$$\lambda^< = \lambda, \quad (C2)$$

$$\lambda_1^< = \lambda_1, \quad (C3)$$

$$D^< = D. \quad (C4)$$

We now rescale space, time and fields so as to raise the upper wavevector cutoff back to Λ . This gives the following differential RG flow equations for ν and g :

$$\begin{aligned} \frac{d\nu}{dl} = & \nu \left[z - 4 + \left\{ \frac{\lambda^2 D}{\nu^3} \frac{6-d}{4d} - \frac{\lambda_1^2 D}{\nu^3} \right. \right. \\ & \left. \left. + \frac{\lambda_1^2 D}{\nu^3 d} \left(\frac{6-d}{4} - \frac{6}{d+2} + 3 \right) \right\} \right] \end{aligned}$$

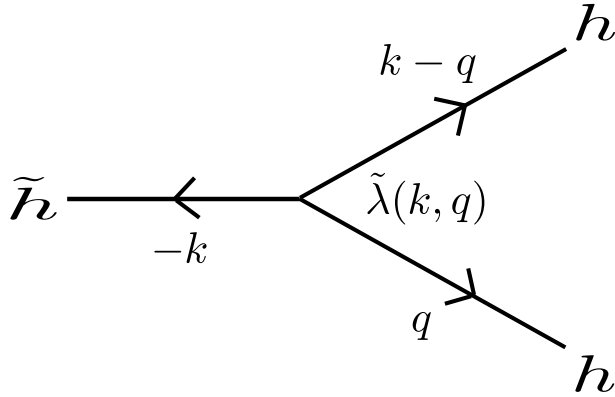


FIG. 4: Effective vertex $\tilde{\lambda}(\mathbf{k}, \mathbf{q}) = -\frac{1}{2}[q^2 \mathbf{k} \cdot (\mathbf{k} - \mathbf{q}) + (\mathbf{k} - \mathbf{q})^2 \mathbf{k} \cdot \mathbf{q}]$.

$$\begin{aligned}
 & + \frac{\lambda \lambda_1 D}{\nu^3} \Big\} K_d \Lambda^{d-4} \Big], \\
 \frac{dg}{dl} &= g \left[4 - d - 3 \left\{ \frac{\lambda^2 D}{\nu^3} \frac{6-d}{4d} - \frac{\lambda_1^2 D}{\nu^3} \right. \right. \\
 & \quad \left. \left. + \frac{\lambda_1^2 D}{\nu^3 d} \left(\frac{6-d}{4} - \frac{6}{d+2} + 3 \right) \right. \right. \\
 & \quad \left. \left. + \frac{\lambda \lambda_1 D}{\nu^3} \right\} K_d \Lambda^{d-4} \right].
 \end{aligned} \tag{C5}$$

$$\begin{aligned}
 & + \frac{\lambda_1^2 D}{\nu^3 d} \left(\frac{6-d}{4} - \frac{6}{d+2} + 3 \right) \\
 & + \frac{\lambda \lambda_1 D}{\nu^3} \Big\} K_d \Lambda^{d-4} \Big].
 \end{aligned} \tag{C6}$$

This clearly shows that $d = 4$ is the critical dimension of g . Near $d = 4$, (C6) reduces to (10) of the main text.

The Feynman diagrams in Fig. 3 can be used to calculate ν_{eff} , whence the wavevector loop integrals are done from Λ all the way to $2\pi/L$. Clearly for $d < 4$, the wavevector loop integrals depend sensitively on L , the system size. In fact, they diverge with L , a fact that opens up the intriguing possibility of crumpling with increasing L . In contrast, these wavevector integrals remain finite for $d > 4$, even if $L \rightarrow \infty$ limit is taken.

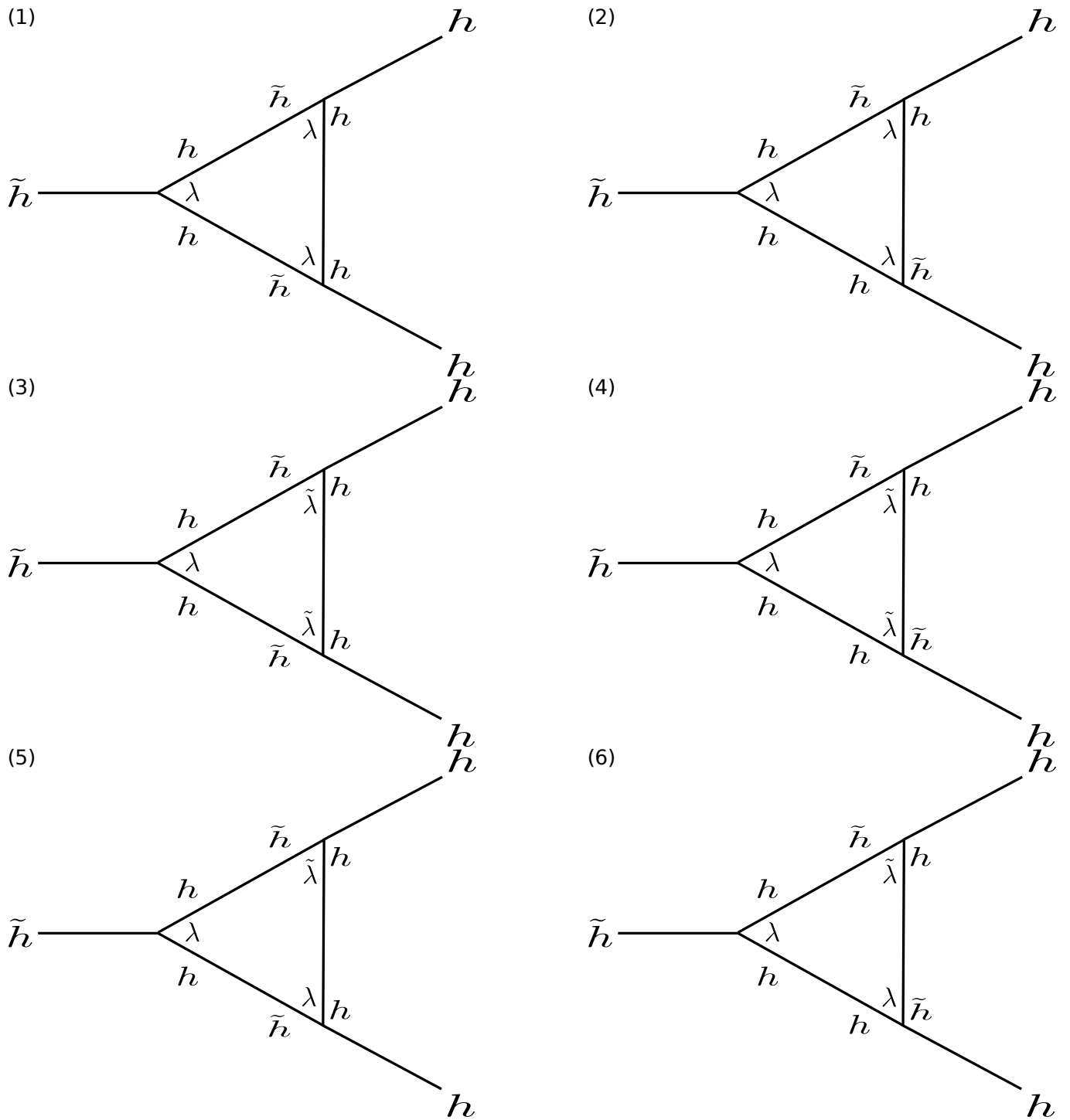


FIG. 5: One-loop Feynman diagrams which contribute to the fluctuation-corrections of λ .

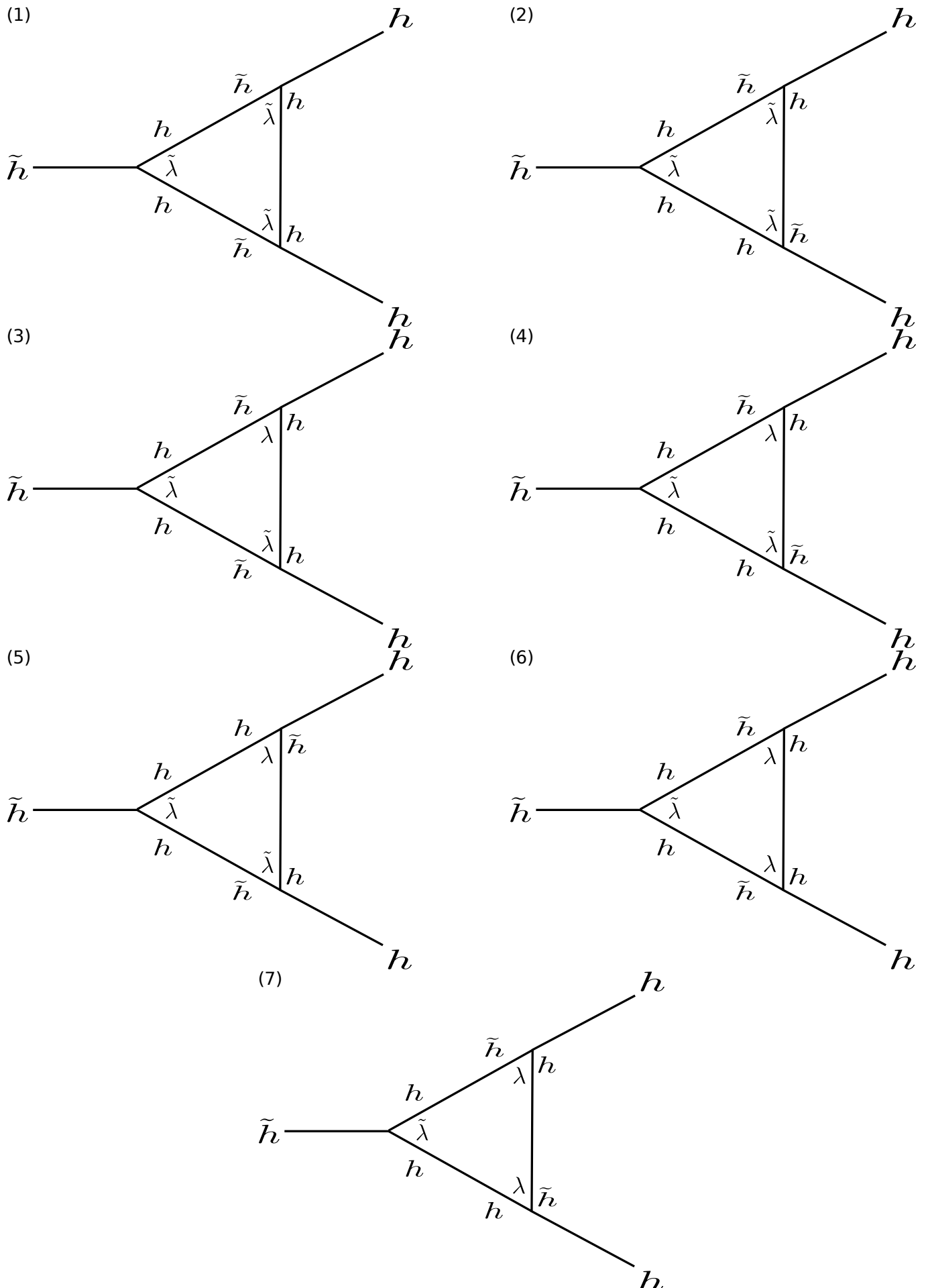


FIG. 6: One-loop Feynman diagrams which contribute to the fluctuation-corrections of $\tilde{\lambda}$.